



FORCED AND NATURAL CONVECTION

Forced and natural convection	1
Curved boundary layers, and flow detachment.....	1
Forced flow around bodies.....	3
Forced flow around a cylinder	3
Forced flow around tube banks.....	5
Forced flow around a sphere.....	6
Pipe flow	7
Entrance region	7
Fully developed laminar flow	8
Fully developed turbulent flow	10
Reynolds analogy and Colburn-Chilton's analogy between friction and heat flux.....	11
Empirical correlations for forced convection.....	12
Natural convection	14
Boundary layer on a hot vertical plate	14
Empirical correlations for natural convection.....	17
Heat transfer fluids.....	19
Air and other permanent gases.....	20
Water.....	20
Water antifreeze mixtures	20
Silicone oils.....	20
Hydrocarbon oils.....	20
Fluorocarbon oils	21
Phase-change fluids. Refrigerants.....	21
Liquid metals.....	21
Nanofluids.....	21

FORCED AND NATURAL CONVECTION

Curved boundary layers, and flow detachment

[Heat and Mass Transfer](#) by convection is here focused on heat and mass flows at walls. After a general [introduction to convection, and the basic boundary layer modelling](#), we proceed with the analysis of heat and mass convection over curved surfaces, what shows a new key feature, the longitudinal pressure-gradient implied by the curvature, which may cause detachment of the boundary layer, becoming a free shear layer that forms a wake behind the object; recall that most practical fluid flows are high-Reynolds-number flows (due to the low viscosity of air and water), which are modelled (since the seminal work of

Prandtl in 1904) as an inviscid external flow plus a viscosity-dominated flow confined within some thin shear layers, either bounded to solids, or free-moving within the fluid.

If we start with zero-incidence (a sharp solid surface aligned with the flow, Fig. 1), and consider the effect of a smooth curvature bending downwards (convex surface from the top, concave surface from the bottom), the external flow (outside the boundary layer) will accelerate over a concave surface (to keep the same flow-rate with a converging cross-section area, like in a nozzle), and will decelerate over a convex surface (to keep the same flow-rate with a diverging cross-section area, like in a diffuser). We are considering only subsonic flow.

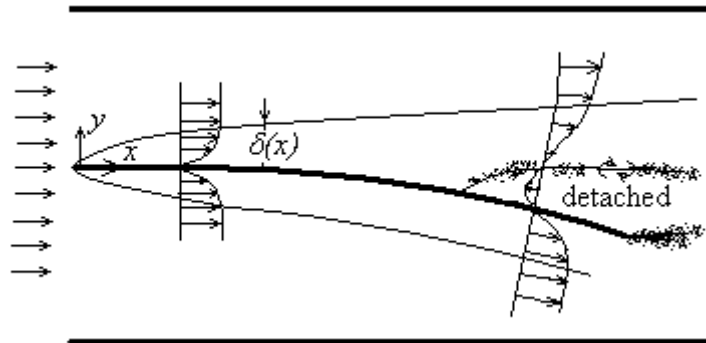


Fig. 1. Boundary layer flow over a curved thin plate with zero incidence, to see the development of a diverging flow (upper side) and a converging flow (lower side). It is shown within a rectangular channel just to emphasize the change in cross-flow area.

The pressure-gradients in the external flow automatically transmit to the boundary layer, since the transversal momentum equation [showed](#) that the transversal pressure-gradient within the boundary layer is negligible. If the pressure-gradient is favourable (i.e. causing the fluid to accelerate, what corresponds to a negative gradient) there is no big changes: the local Reynolds number increases so the boundary layer thins, increasing the wall gradients (i.e. increasing both the shear stress and the convective coefficient), and causing laminar-to-turbulent transition earlier downstream than over a flat plate. If the pressure-gradient is adverse (i.e. positive, as in the upper part of Fig. 1, causing the fluid to decelerate) there can be a big change: the local Reynolds number decreases so the boundary layer thickens, decreasing the wall gradients. The deceleration imposed by the external pressure-gradient in this latter case may cause the boundary-layer flow to reverse, since within the boundary layer, the velocity must decrease by mechanical energy dissipation by friction, e_{mdf} (which would force the flow to stop), on top of which is the retardation caused by the pressure-gradient, as explained by the modified Bernoulli equation:

$$\nabla \left(p + \frac{1}{2} \rho v^2 \right) + e_{mdf} = 0 \quad \rightarrow \quad \underset{>0}{\nabla p} + \frac{1}{2} \rho \underset{>0}{\nabla (v^2)} + e_{mdf} = 0 \quad (1)$$

Flow separation causes local pulsating flows and forces in a closed reattachment region (before the wake detaches, see Fig. 1), with great heat-transfer enhancement, but also with a sharp increase in wake thickness and drag, and loss of transversal suction (lift force).

Flow separation renders the analytical modelling of momentum, heat, and mass flows over bodies intractable except in very slender cases (blades and foils), and, although the numerical simulation using commercial CFD packages gives nowadays accurate predictions in many cases, empirical correlations are still widely used in analysis and design.

Forced flow around bodies

In all practical cases of flow around bodies, there is flow detachment and turbulence, preventing a detailed analysis and forcing an empirical approach. When the body is so streamlined that there is no flow separation, as in aerodynamic airfoils, [boundary-layer modelling](#), accounting for curvature, is good enough to compute transfer rates of momentum (viscous drag), energy (heat) convection, or mass convection. The other extreme case without flow separation is in the viscosity-dominated flow at very low Reynolds numbers, as in the Stokes flow. Thus, in all practical cases of flow around bodies, one has to resort to empirical correlations for convection analysis.

The most common configurations of forced flow around blunt bodies (to be further analysed below) are:

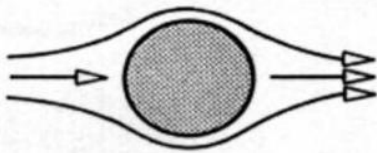
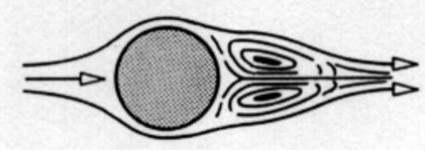
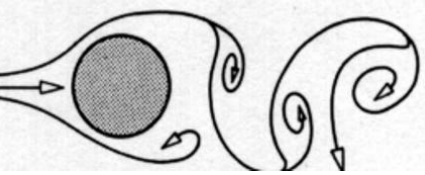
- Flow around a circular cylinder.
- Flow around tube banks.
- Flow around a sphere.

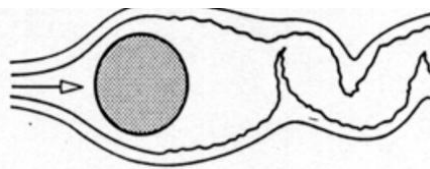
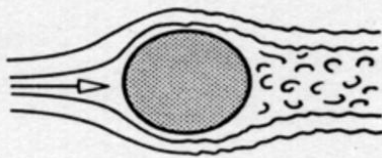
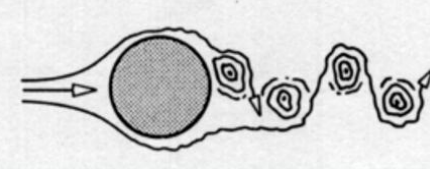
Many other correlations for two-dimensional and tri-dimensional objects have been developed and can be found in the literature; e.g. flow around triangular or square bars at different angles, flow around hemispheres or caps, etc.

Forced flow around a cylinder

The flow past a two-dimensional cylinder in a uniform stream is one of the most studied problems in fluid mechanics. The different flow regimes in terms of relative velocity for the flow across a cylinder are presented in Table 1.

Table 1. Main flow regimes for flow across a cylinder.

$0 < Re_D < 5$		Un-separated streaming flow, also named creeping or Stokes flow.
$5 < Re_D < 40$		A pair of symmetric vortices appears, counter-rotating and fixed in the wake, with their elongation growing with Re_D .
$40 < Re_D < 150$		A laminar boundary layer detachment by periodic vortex shedding of eddies from alternating sides at a frequency f_K (drag force pulsates at $2f_K$) given by the relation $St = f(Re)$, with the Strouhal number $St = f_K D / V = 0.2 \pm 0.02$ for $10^2 < Re_D < 10^5$. Named Kármán vortex street.

$150 < Re_D < 3 \cdot 10^5$		<p>The boundary layer is laminar up to the separation point (at the front); the vortex street is turbulent, and the wake flow field is increasingly three-dimensional. At $Re_D = 3 \cdot 10^5$, Strouhal number shows scatter in the range $St = 0.18..0.28$.</p>
$3 \cdot 10^5 < Re_D < 3.5 \cdot 10^6$		<p>The laminar boundary layer undergoes transition to a turbulent boundary layer before separation, which now is at the rear; the wake becomes narrower and disorganized.</p>
$3.5 \cdot 10^6 < Re_D$		<p>A turbulent vortex street is re-established, but it is narrower than was the case for $150 < Re_D < 3 \cdot 10^5$.</p>

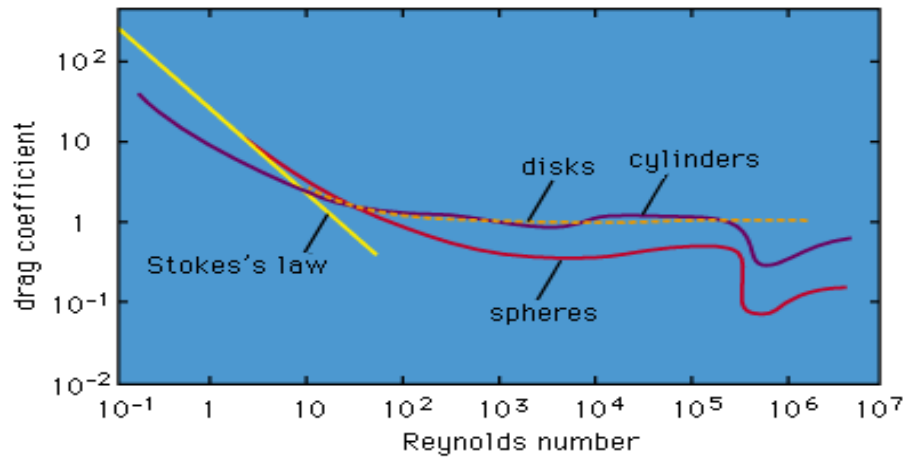
Heat transfer around a circular cylinder can be modelled by the correlation (Churchill-Bernstein-1977):

$$Nu_D = 0.3 + \frac{0.62 Re_D^{1/2} Pr^{1/3}}{\left[1 + (0.4/Pr)^{2/3}\right]^{1/4}} \left[1 + \left(\frac{Re_D}{282000}\right)^{5/8}\right]^{4/5} \quad (2)$$

good for $10^2 < Re_D < 10^7$ and $Pe = Re_D Pr > 0.2$. Azimuthally, Nu_θ is highest at 110° and lowest at 80° (from leading point). Ref.: Churchill, S.W. y Bernstein, M., A correlating equation for forced convection from gases and liquids to a circular cylinder in cross-flow. J. Heat transfer. Vol. 99, pp. 300-306, 1977. For hot wire velocimetry in gases (in the range $1 < Re_D < 1000$), a simple correlation $Nu_D = (2 + \sqrt{Re_D})/3$, similar to the pioneering correlation by King in 1914, may be good enough, although better fittings exists (e.g. Collis & Williams, 1959, J. Fluid Mech. 6, pp. 357-384).

Drag force around a circular cylinder varies with flow speed as shown in Fig. 2 and can be approximated as follows:

Re_D range	c_D	Comments
$Re_D < 10$	$c_D = 8\pi / (Re_D(2 - \ln Re_D))$	Lamb approximation to Stokes flow for slow laminar motion (creeping flow). Stokes paradox: no solution to the low-Reynolds number Navier-Stokes equations can be found which satisfies the boundary conditions at the surface and at infinity. See below the exact solution for a sphere.
$10 < Re_D < 4 \cdot 10^5$	$c_D = 1$	Newton law of constant drag coefficient.
$Re_D > 4 \cdot 10^5$	$c_D = 0.3$	Turbulent transition depends on the turbulence intensity of the stream; it is $Re_D = 2 \cdot 10^5$ for $i_u = v'_{rms}/v = 1$, but drops to $2 \cdot 10^4$ for $i_u = 10$ and may reach $4 \cdot 10^5$ for $i_u = 0.1$.



©1994 Encyclopaedia Britannica, Inc.

Fig. 2. Drag coefficient, c_D , for a cylinder, a disc, and a sphere. Drag force is $F_D = c_D A \frac{1}{2} \rho v^2$.

Forced flow around tube banks

A tube bank, or tube bundle, is an array of parallel tubes (circular or not) exposed to a transversal flow (perpendicular or not). Tube-bank geometry is characterised by layout (see Fig. 3), and longitudinal and transversal pitch (separation between centres), with s_h being the longitudinal pitch (i.e. along the flow), and s_v transversal pitch, for both, in-line, and staggered geometries. At least 6 tubes per transversal row, with tube slenderness $L/D > 5$, are usually assumed to avoid the need of end-effects corrections.

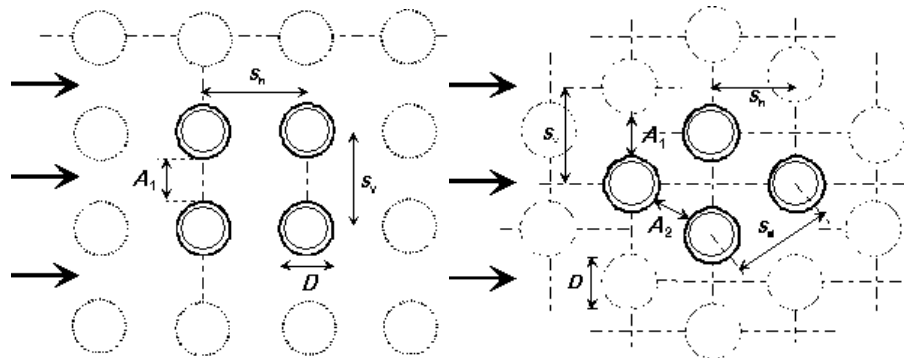


Fig. 3. In-line and staggered tube-bank arrangements.

Heat transfer in tube banks can be computed from the general correlation (Zukauskas-1987):

$$Nu_D = C_1 C_2 Re_{D,\max}^n Pr^m (Pr/Pr_s)^{0.25} \quad (3)$$

good for $0.7 < Pr < 500$ and $1 < Pr/Pr_s < 3.2$, where C_1 depends on the number of rows N_{rows} as:

	$N_{\text{rows}}=1$	2	3	4	5	7	10	13	>16
In-line	0.70	0.80	0.86	0.90	0.93	0.96	0.98	0.99	1
Staggered	0.64	0.76	0.84	0.89	0.93	0.96	0.98	0.99	1

and C_2 , n and m depend on layout and flow regime as:

<i>Bank type</i>	Re_D range	C_2	n	m
In-line	$0 < Re < 10^2$	0.9	0.4	0.36
In-line	$10^2 < Re < 10^3$	0.52	0.5	0.36
In-line	$10^3 < Re < 2 \cdot 10^5$	0.27	0.63	0.36
In-line	$2 \cdot 10^5 < Re < 2 \cdot 10^6$	0.033	0.8	0.4
Staggered	$0 < Re < 5 \cdot 10^2$	1.04	0.4	0.36
Staggered	$5 \cdot 10^2 < Re < 10^3$	0.71	0.5	0.36
Staggered	$10^3 < Re < 2 \cdot 10^5$	$0.35(s_v/s_h)^{0.2}$	0.6	0.36
Staggered	$2 \cdot 10^5 < Re < 2 \cdot 10^6$	$0.031(s_v/s_h)^{0.2}$	0.8	0.36

Parameters in (3) must be evaluated at the mid input/output temperature, except for Pr_s , that should be evaluated at the tube surface. Besides, in the computation of the Reynolds number in (3), $Re_{D,\max} = v_{\max} D / \nu$, the maximum flow speed, v_{\max} , should be used:

<i>Bank type</i>	Maximum speed
In-line	$v_{\max} = \left[s_v / (s_v - D) \right] v_{\infty}$
Staggered, with $\left[s_h^2 + (s_v/2)^2 \right]^{1/2} < (s_v + D)/2$	$v_{\max} = \left[s_v / (s_d - D) \right] v_{\infty}$
Staggered, with $\left[s_h^2 + (s_v/2)^2 \right]^{1/2} > (s_h + D)/2$	$v_{\max} = \left[s_v / (s_v - D) \right] v_{\infty}$

If the tube bank is slanted an angle θ perpendicular to the flow direction, the same correlations can be applied if the obtained Nusselt number, Nu , from (3) is multiplied by $\sin(\theta)^{0.6}$ to account for the tilting. The effect of finned tubes may be also taken into account by adding to the naked-tube area the fin-root area multiplied by the fin efficiency.

Ref.: Zukauskas, A. "Heat transfer from tubes in cross flow", in Handbook of single phase convective heat transfer, Wiley Interscience, 1987.

Forced flow around a sphere

Heat transfer around a sphere can be modelled by the correlation (Whitaker-1972):

$$Nu_D = 2 + \left(0.4 Re_D^{1/2} + 0.06 Re_D^{2/3} \right) Pr^{2/5} \left(\mu / \mu_w \right)^{1/4} \quad (4)$$

good for $3.5 < Re_D < 7.6 \cdot 10^4$, $0.7 < Pr < 380$, and $1 < \mu / \mu_w < 3.2$, with all properties evaluated at T_{∞} except μ_w at T_w . Ref.: Whitaker S., Forced convection heat transfer correlations for flow in pipes, past flat plates, single cylinders, single spheres and for flow in packed beds and tube bundles. AIChE Journal, Vol. 18, pp. 361-371, 1972.

Notice that $Nu_D \rightarrow 2$ for low Reynolds numbers (and the same happens in the natural convection case, see below). In fact, this is the limit of no convection, i.e. of pure heat conduction through the fluid, with a temperature field $T(r) = T_{\infty} + (T_w - T_{\infty})R/r$ and hence $\dot{q} = h(T_w - T_{\infty}) = -k(dT/dr)_{r=R} = k(T_w - T_{\infty})/R$, with the result that $Nu_D = hD/k \rightarrow 2$ in spite of the common saying that Nu is the ratio of convective to conductive heat transfer (it is $Nu_R = hR/k \rightarrow 1$). Notice also that Nu being finite, h is proportional to $1/R$ and approaches infinite as $D \rightarrow 0$.

For a falling drop, and for droplets from injectors, $Nu_D = 2 + 0.6Re_D^{1/2}Pr^{1/3}$ is often used. Notice that, in absence of convection, $Nu_D=2$ for a sphere in a heat-conducting media, as can easily be analytically-deduced.

Flow drag on a sphere was presented in Fig. 2, and can be modelled as:

Re_D range	c_D	Comments
$Re_D < 1$	$c_D = 24/Re_D$	Stokes law, $F_D = 3\pi\mu DV$, for slow laminar motion (creeping flow).
$2 < Re_D < 500$	$c_D = 18.5/Re_D^{0.6}$	Intermediate regime
$500 < Re_D < 3 \cdot 10^5$	$c_D = 0.44$	Newton law of constant drag coefficient.
$Re_D > 4 \cdot 10^5$	$c_D = 0.1$	Drag reduction in a smooth sphere due to turbulent transition. Transition depends on surface roughness and on the turbulence intensity of the stream (it is $Re_D = 2 \cdot 10^5$ for $i_u \equiv v'_{rms}/v = 1$, and drops to $2 \cdot 10^4$ for $i_u = 10$ (e.g. in a golf ball), and may reach $4 \cdot 10^5$ for $i_u = 0.1$).

There are other forced-flow configurations of interest in heat and mass transfer, which have been studied and correlations are available, as for flows through packed beds, impinging jets (free or submerged, gas or liquid; e.g. Webb & Ma-1995), etc.

Pipe flow

Heat and Mass Transfer by convection focuses on heat and mass flows at walls; so that, after the unbiased case of the [forced flow over a flat plate presented aside](#), and the effects of curved boundary layers around bodies considered above, we deal now with heat and mass convection at internal walls of pipes and tubes due to an imposed fluid flow along them.

The baseline configuration for the analytical and numerical-correlation studies of momentum, heat, and mass transfer in pipes and ducts corresponds to the circular pipe, what can be extrapolated to non-circular cylindrical pipes and ducts if an equivalent diameter is used, named hydraulic diameter and defined by:

$$D_h \equiv \frac{4A}{p} \stackrel{\substack{A=\pi D^2/4 \\ p=\pi D}}{=} D \quad (5)$$

A being the cross-section area and p its perimeter.

Entrance region

The entrance region to a pipe is the region where the fluid changes from the usually quiescent state in the supplying reservoir, to fully-developed flow downstream along the pipe. Neglecting the three-dimensional effects of sucking (and a possible flow-detachment at the pipe-lips), we may consider as a model of the entrance region that of a uniform forced flow interacting with the duct wall, which, for radius-of-curvature of the duct-cross-section shape larger than the boundary-layer thickness, can be

approximated by forced flow over a flat plate, until the boundary-layers from different walls meet at the centre of the duct, which, for cylindrical ducts, will occur when the boundary-layer-thickness, δ , equals the radius of the pipe, $D/2$, i.e. according to [Table 4 aside](#), up to:

$$\frac{\delta}{x} = \frac{4.92}{(\nu x/\nu)^{1/2}} \rightarrow \frac{L_e}{D} = 0.01 Re_D \quad (6)$$

for laminar entrance, to be doubled because now Re_D is defined in terms of the mean velocity, u_m , from $\dot{m} = \rho u_m A$, instead of the maximum velocity (as explained below). By the way, Reynolds numbers in pipe flow can be computed in terms of mass-flow-rates as $Re_D \equiv uD/\nu = 4\dot{m}/(\pi D\mu)$, $\mu = \rho\nu$ being the dynamic viscosity of the fluid.

The correlation most used to compute the entrance length in laminar flow is, however:

$$\frac{L_e}{D} = 0.05 Re_D \quad (7)$$

i.e. in the usual limit $Re_D=2300$, $L_e/D \approx 100$ (e.g., 1 m for a 1 cm pipe with viscous flow; mind that this is not the common case, since for water at >0.5 m/s and for air at >7 m/s, the entrance boundary layer becomes turbulent at 1 m downstream). For turbulent flow, the same procedure ([Table 4 aside](#)) yields:

$$\frac{\delta}{x} = \frac{0.38}{(\nu x/\nu)^{1/5}} \rightarrow \frac{L_e}{D} = 1.41 Re_D^{1/4},$$

but $\frac{L_e}{D} = 1.36 Re_D^{1/4} \approx 10$ is used for turbulent entrance. (8)

e.g., for a typical value of $Re_D=10^4$, $L_e/D \approx 14$ (that is why a value $L_e/D \approx 10$ is commonly used as a rough estimation, because the growth is small: e.g. for $Re_D=10^6$, $L_e/D \approx 40$).

A thermal-entry-length and a solutal-entry-length are defined in a similar way. In the laminar case, the correlations most used are $L_{e,th}/D = 0.05 Re_D Pr$ and $L_{e,sol}/D = 0.05 Re_D Sc$ (Kays & Crawford 1993), whereas in the turbulent case, the same expression (8) is used for all entry lengths: hydrodynamic, thermal, and solutal, since all transfers are dominated by the large eddy convection and not by diffusion details.

It should be noted that both, friction and heat convection (and solutal), are enhanced at the entry region, because of the much higher velocity and temperature (and concentration) gradients there. Heat-convection correlations for laminar and turbulent flows in pipes are jointly presented further down in Table 2, but some theoretical analysis is developed first.

Fully developed laminar flow

It was found by Reynolds in 1883 that the developed flow in a straight circular pipe is laminar up to at least $Re_D=2300$, with transition flow in the range $2000 < Re_D < 10\,000$, or, most of the times between $2300 < Re_D < 4000$ (always depending on wall smoothness, details in entrance geometry, initial turbulence

level, noise...), and being fully turbulent beyond. Transition to turbulence is delayed in curved pipes due to the stabilising contribution of the secondary flow generated by centrifugal forces.

It can easily be deduced (as follows), that the velocity profile in steady laminar flow is parabolic. Taking a centred fluid cylinder up to radius $r < R \equiv D/2$, the force balance gives:

$$\pi r^2 dp + \tau 2\pi r dx = 0 \xrightarrow{\tau = \mu dv/dr} du = \frac{-r}{2\mu} dr \frac{dp}{dx} \xrightarrow{u(R)=0} u(r) = \frac{R^2 - r^2}{4\mu} \frac{dp}{dx} \quad (9)$$

from where the area-average speed is:

$$u_m \equiv \frac{1}{\pi R^2} \int_0^R u 2\pi r dr = \frac{R^2}{8\mu} \frac{dp}{dx} = \frac{u(r)_{r=0}}{2} = \frac{u_0}{2} \quad (10)$$

and the gradient at the wall $du(r)/dr|_{r=R} = 4u_m/R$. Equation (9) relates the mean flow-speed with the pressure gradient, although the standard way of presenting pressure-loss data is in terms of the dynamic pressure of the flow ($1/2\rho v^2$) and a pressure-loss coefficient c_K , which for long pipes is recast as $\lambda L/D$:

$$\Delta p_t = c_K \frac{1}{2} \rho u_m^2 \stackrel{\text{pipes}}{=} \lambda \frac{L}{D} \frac{1}{2} \rho u_m^2 \quad \text{with} \quad \lambda = \frac{64}{Re_D} \quad (\text{Poiseuille law for laminar flow}) \quad (11)$$

The temperature profile can also be easily obtained from the energy balance of an elementary cylindrical shell of length dx and radii between r and $r+dr$, and its integration. For a constant heat flux at the pipe wall, temperature must grow linearly with pipe length according to a longitudinal energy balance; thence:

$$\rho c \frac{DT}{Dt} = u(r) \rho c \frac{\partial T}{\partial x} = \left(1 - \frac{r^2}{R^2}\right) u_0 \rho c \frac{\partial T}{\partial x} = k \nabla^2 T = k \frac{1}{r} \frac{\partial}{\partial r} \left(r \frac{\partial T}{\partial r} \right) \xrightarrow{\partial T/\partial x = \text{const}} \quad (12)$$

$$T(r, x) = T_0(x) + \frac{\partial T}{\partial x} \frac{u_0 R^2}{4a} \left[\left(\frac{r}{R}\right)^2 - \frac{1}{4} \left(\frac{r}{R}\right)^4 \right],$$

$$\text{with} \quad \begin{cases} T_w(x) = T(r, x)|_{r=R} = T_0(x) + \frac{3u_0 R^2}{16a} \frac{\partial T}{\partial x} \\ \left. \frac{\partial T}{\partial r} \right|_{r=R} = \frac{u_0 R}{4a} \frac{\partial T}{\partial x} \end{cases}$$

where the longitudinal temperature gradient $\partial T/\partial x$ would be positive for heating (i.e. when the fluid is heated), and negative for cooling. As representative temperature at a cross-section, the 'mixing-cup average' or 'bulk temperature', defined by:

$$T_b \equiv \frac{\int_0^R u(r) \rho c T(r) 2\pi r dr}{\int_0^R u(r) \rho c 2\pi r dr} \quad (13)$$

is used, since the interest is in the energy balance, $\dot{Q} = hA(T_{w,mean} - T_{b,mean}) = \dot{m}c dT/dx = \int (\rho u(r) 2\pi r dr) c (dT(r)/dx)$. In the present case of laminar flow:

$$\begin{aligned} T_b &\equiv \frac{\int_0^R u(r) \rho c T(r) 2\pi r dr}{\int_0^R u(r) \rho c 2\pi r dr} = \frac{\int_0^R \left(1 - \frac{r^2}{R^2}\right) u_0 \rho c T(r) 2\pi r dr}{u_m \rho c \pi R^2} \rightarrow \\ &\rightarrow T_b(x) = T_0(x) + \frac{7}{96} \frac{u_0 R^2}{a} \frac{dT}{dx} = T_0(x) + \frac{7}{48} \frac{u_m R^2}{a} \frac{dT}{dx} = T_w(x) - \frac{11}{48} \frac{u_m R^2}{a} \frac{dT}{dx} \end{aligned} \quad (14)$$

Thus, Newton's law of cooling, $\dot{q} \equiv h(T - T_\infty) = -k \nabla_n T$, applied to our heat-convection problem in pipes, gives:

$$\begin{aligned} \dot{q} &\equiv h(T_w - T_b) = -k \left. \frac{\partial T}{\partial y} \right|_{y=0} = k \left. \frac{\partial T}{\partial r} \right|_{r=R} = h \frac{11}{48} \frac{u_m R^2}{a} \frac{dT}{dx} = k \frac{u_m R}{2a} \frac{\partial T}{\partial x} \rightarrow \\ &\rightarrow h = \frac{24}{11} \frac{k}{R} \Rightarrow Nu_D = \frac{48}{11} = 4.36 \end{aligned} \quad (15)$$

If, instead of a constant heat flux along the pipe walls, a constant wall temperature were assumed, the result would have been $Nu_D = 3.66$. An order of magnitude analysis of the heat equation, $u \rho c \partial T / \partial x = a \partial^2 T / \partial y^2$, and the energy balance equation, $\dot{m} c \partial T / \partial x = \rho u (\pi D^2 / 4) c \partial T / \partial x = h \pi D \Delta T$, would have provided already a Nu_D -value of order unity.

A final remark on laminar flow in pipes is that the temperature profile (the associated viscosity change) gives way to a small distortion of the parabolic velocity profile of isothermal laminar flows, making it more flat in the case of liquid heating (or gas cooling), or more lobe-like in the case of liquid cooling (or gas heating).

Fully developed turbulent flow

Turbulent flow is more difficult to model. Little more than Reynolds analogy between friction and heat convection, $Nu = (c_f / 2) Re$, (or $Sh = (c_f / 2) Re$ for solutal convection) can be analytically deduced, what is not meagre, since measurements of pressure loss in pipes (not difficult to perform) then allow the computation of thermal and solutal transfer rates. Reynolds analogy is based on the similarity between momentum, heat, and mass transfer from the general balance equations:

$$\frac{D\vec{v}}{Dt} \stackrel{\nabla p=0}{=} \nu \nabla^2 \vec{v}, \quad \frac{DT}{Dt} \stackrel{\phi=0}{=} a \nabla^2 T, \quad \frac{Dy_i}{Dt} \stackrel{w_i=0}{=} D_i \nabla^2 y_i \rightarrow \frac{1}{\nu} \frac{\nabla v}{v} = \frac{1}{a} \frac{\nabla T}{\Delta T} = \frac{1}{D_i} \frac{\nabla y_i}{\Delta y_i} \quad (16)$$

which, with the definitions of λ (or f , the Darcy or Moody friction factor, not to be confused with c_f , the Fanning factor):

$$\Delta p_t \equiv \lambda \frac{L}{D} \frac{1}{2} \rho v^2, \quad \tau \equiv c_f \frac{1}{2} \rho v^2, \quad F_f = \Delta p_t \frac{\pi D^2}{4} = \tau \pi D L \Rightarrow \lambda = 4c_f \quad (17)$$

and the definition of the convective coefficients, finally yields:

$$\left. \begin{aligned} Nu &\equiv \frac{hD}{k}, \quad h = \frac{k \nabla T|_w}{\Delta T} \Rightarrow a \frac{\nabla T|_w}{\Delta T} = a \frac{Nu}{D} \\ c_f &\equiv \frac{\tau}{\frac{1}{2} \rho v^2} = \frac{\mu \nabla v|_w}{\frac{1}{2} \rho v^2} \Rightarrow v \frac{\nabla v|_w}{v} = v \frac{vc_f}{2v} \end{aligned} \right\} \frac{a \frac{\nabla T}{\Delta T}}{v \frac{\nabla v}{v}} = 1 = \frac{a \frac{Nu}{D}}{v \frac{vc_f}{2v}} = \frac{Nu}{\frac{c_f}{2} Re Pr} \quad (18)$$

known as modified Reynolds analogy, $Nu = (c_f/2) Re Pr = (\lambda/8) Re Pr$. However, the most used Pr -correction to Reynolds analogy is Colburn-Chilton analogy.

Reynolds analogy and Colburn-Chilton's analogy between friction and heat flux

As just stated above, Osborne Reynolds, in 1874, was the first to make use of the mathematical similarity between the momentum equation and the energy equation in convection. However, the most widely used analogy is the one due to Colburn and Chilton (1934):

$$\boxed{Nu_D = \frac{\lambda}{8} Re_D Pr^{1/3}}, \text{ and similarly } \boxed{Sh_D = \frac{\lambda}{8} Re_D Sc^{1/3}}. \quad (19)$$

because this Prandtl-number correction is more accurate than the one from (18), as was [deduced before, for the laminar boundary layer over a flat plate.](#)

The friction factor for fully developed flow in circular pipes, as a function of Reynolds number Re_D and relative wall roughness, ε/D , is shown in Fig. 4, first presented by L.F. Moody, in 1944 (e.g. $\varepsilon \approx 2 \cdot 10^{-6}$ m in glass or plastic pipes, $\varepsilon \approx 0.1 \cdot 10^{-3}$ m in uncoated steel and galvanised iron, or $\varepsilon \approx 1 \cdot 10^{-3}$ m in concrete). This can be applied to non-circular ducts by using the equivalent hydraulic diameter: $D_h = 4A/p$. Notice that instead of the Darcy friction factor λ , the Fanning friction factor $c_f = \lambda/4$ is often used, and sometimes a so-called Colburn j -factor, $j \equiv c_f/2$; as it might appears that the symbol f is used in some texts for the Fanning friction factor and in some others for the Darcy friction factor, it is suggested to always make a quick check, for instance on the laminar friction factor in pipes (Hagen-Poiseuille equation), that reads $\lambda = 64/Re$ or $c_f = 16/Re$, according to which of the definitions in (17) is used.

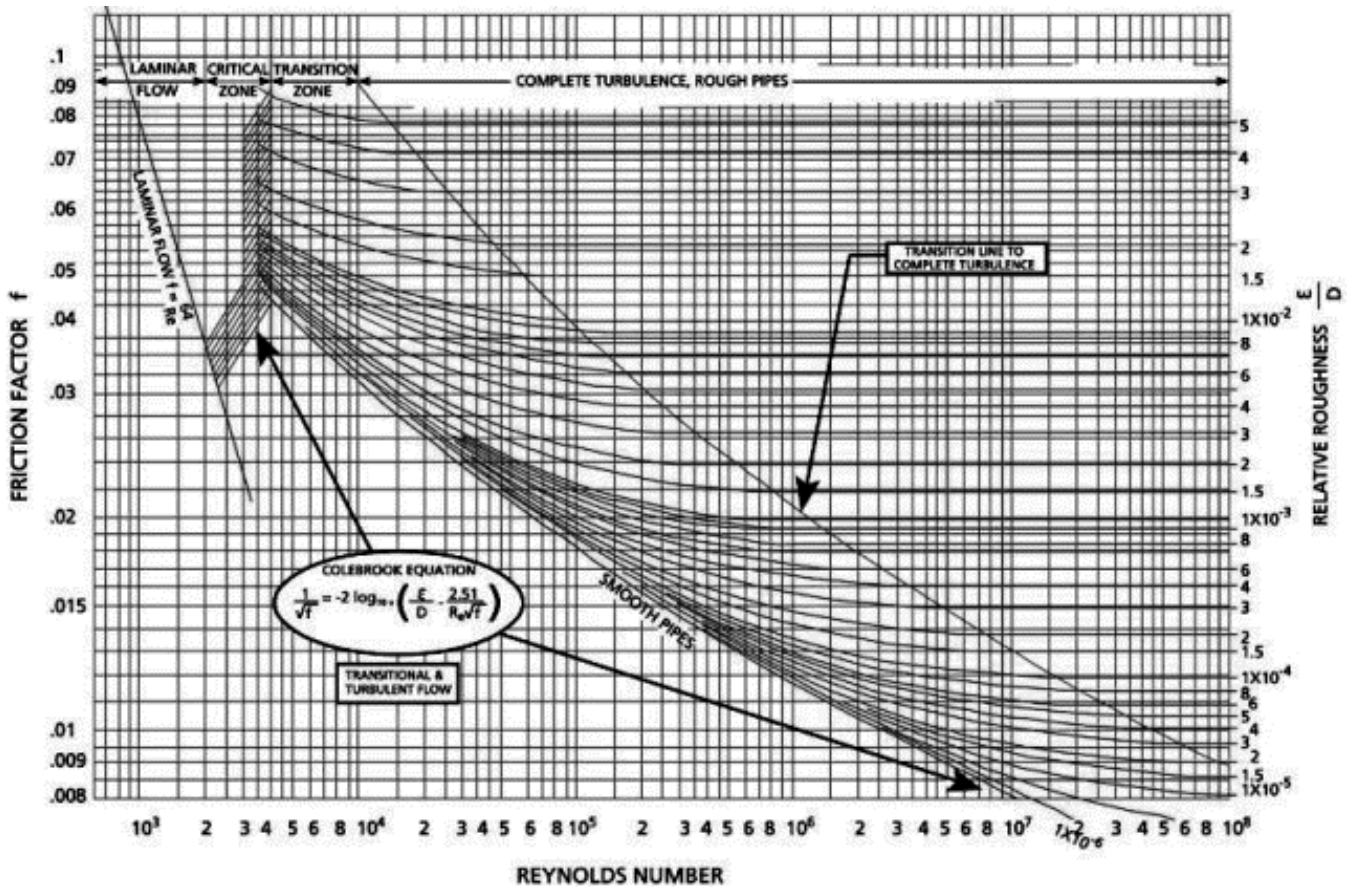


Fig. 4. Darcy friction factor f (also named λ) for fully developed flow in circular pipes (Moody diagram).

Some empirical correlations for fully-developed forced-flow in pipes and ducts are compiled in Table 2 for both, friction factor, and heat convection; fluid properties should be evaluated at an average bulk temperature (mean value between inlet and outlet values), but they are often evaluated with inlet values (and later iterated, if any, after outlet values have been computed). The required pumping power to force the flow can be computed from $\dot{W} = \dot{m}\Delta p / (\rho\eta_p)$, with η_p being the pump efficiency, and $\Delta p = c_K(1/2)\rho v^2$ being the total pressure loss in the circuit; the global pressure-loss coefficient $c_K = \lambda L/D + \sum c_{K,i}$ should account for the whole pipe length, L , plus every flow restriction, $c_{K,i}$: bends, valves, filters, change of diameter or shape (including suction from or discharge to reservoirs).

Empirical correlations for forced convection

We here restrict to internal pipe flow; flow around bodies have been presented above, and flow over flat plates (forced flow; natural flow is covered here below) can be found under [Boundary layer flow](#).

Table 2. Heat convection correlations for fully-developed forced-flow in pipes.

Configuration	Friction factor (17)	Heat convection
Circular pipe, laminar flow, ($Re_D < 2300$)	Hagen-Poiseuille (1839): $\lambda = \frac{64}{Re_D}$	$Nu_{D,T} = 3.66$, $Nu_{D,q} = 4.36$
	For short pipes (entry length included): $\lambda = \frac{64}{Re_D} + 1.2 \frac{D}{L}$	Sieder-Tate (1936): $Nu_D = 1.86 \left(\frac{D}{L} Re Pr \right)^{1/3} \left(\frac{\mu_b}{\mu_w} \right)^{0.14}$ valid for $Re Pr D/L > 10$ and

	valid for $\frac{L}{D} > \frac{L_e}{D} = 0.05 Re_D$	$\frac{L}{D} > \frac{L_{e,th}}{D} = 0.05 Re_D Pr$
Circular pipe, turbulent flow, ($Re_D > 2300$)	Smooth pipe ($Re_D < 0.2 \cdot 10^6$): $\lambda = \frac{0.32}{Re_D^{1/4}}$	Dittus-Boelter (1930), Colburn (1933): $Nu_D = 0.023 Re_D^{0.8} Pr^n$ $n=0.4$ if $dT_b/dx > 0$, $n=0.3$ for cooling $0.6 < Pr < 160$, $Re_D > 10\,000$ and
	Petukhov (1970): $\lambda = \frac{1}{(0.79 \ln Re_D - 1.64)^2}$	$\frac{L}{D} > \frac{L_{e,th}}{D} = 1.38 Re_D^{1/4}$
	Colebrook (1939): $\frac{1}{\sqrt{\lambda}} = -2 \log_{10} \left(\frac{\varepsilon}{3.7D} + \frac{2.5}{Re_D \sqrt{\lambda}} \right)$	For liquid metals: $Nu_D = 5 + 0.025 (Re_D Pr)^{0.8}$
	Haaland (1983): $\frac{1}{\sqrt{\lambda}} = -1.8 \log_{10} \left(\left(\frac{\varepsilon}{3.7D} \right)^{1.11} + \frac{6.9}{Re_D} \right)$	
	Fully turbulent ($Re_D \varepsilon / D > 3500$): $\frac{1}{\sqrt{\lambda}} = 1.1 - 2 \log_{10} \frac{\varepsilon}{D}$ valid for $\frac{L}{D} > \frac{L_e}{D} = 1.38 Re_D^{1/4}$	
Non-circular pipe, laminar flow, ($Re_D < 2300$)	Square pipe: $\lambda = \frac{57}{Re_D}$	Square pipe: $Nu_{D,T} = 2.98$, $Nu_{D,q} = 3.61$
	Rectangular duct 1:4: $\lambda = \frac{73}{Re_D}$	Rectangular duct 1:4: $Nu_{D,T} = 4.44$, $Nu_{D,q} = 5.33$
	Thin annulus or slots: $\lambda = \frac{96}{Re_D}$	Thin annulus or slots: $Nu_{D,T} = 7.54$, $Nu_{D,q} = 8.24$

One of the most used correlations in heat transfer is the Dittus-Boelter equation: $Nu_D = 0.023 Re_D^{0.8} Pr^n$ (with $n=0.3$ when the fluid cools down, and $n=0.4$ when it heats up), applied to turbulent flow in pipes of $L/D > 10$ at $Re > 10^4$ and $0.6 < Pr < 160$. Why this old correlation (1930) is so much used? The reason is that, although there are other more-precise fittings, this one applies to most practical problems, where pipes are much longer than the diameter, fluids are gases with $Pr \approx 0.7$ or non-metallic liquids (e.g. $Pr=13$ for water at 0°C and $Pr=1.7$ for water at 100°C), and they flow at not too-low speeds (e.g. for a pipe of $D=1$ cm internal diameter, with water flowing at 20°C with a speed of $v=1$ m/s, $Re = vD/\nu = 1 \cdot 0.01/10^{-6} = 10^4$); and, above all, this is a simple equation (explicit and short) with only two parameters, in spite of using floating-point fittings (though sometimes a [4/5 is used instead of 0.8](#) in the Re exponent).

A note on initial and boundary conditions is pertinent. All empirical correlations assume unidirectional steady flow with either constant temperature at the wall or constant heat flux at the wall. In practice, the flow may have some non-one-dimensional components (azimuthal or radial secondary flows, due to entrance effects from bends or obstructions), the flow may be unsteady (e.g. the setup may be heating up), and neither constant temperature nor constant heat flux can be imposed in practice (but a combined heat-transfer problem through the pipe wall with an external fluid or solid environment).

Sometimes, the internal wall of pipes and ducts are intentionally modified, trying to increase heat and mass transfer, for instance by introducing helical ribs or fins. Additionally, the internal wall of pipes and ducts are usually unintentionally modified by dirt growth (fouling) during operation, what imposes an additional resistance to fluid flow, heat transfer, and solutal transfer.

Natural convection

Natural convection is the fluid flow originated by gravity forces acting on non-uniform-density fluids; the density changes may be due to thermal or to solutal gradients. Many different natural-convection configurations are of interest, from the simplest hot/cold vertical plate in a fluid medium, to external convection around hot/cold bodies, or internal convection within hot/cold enclosures (non-isothermal).

Boundary layer on a hot vertical plate

The boundary layer on a hot vertical plate is a canonical thermo-fluid-mechanics problem. A semi-infinite vertical wall is shown in Fig. 5 (it must extend upwards if it is hot, or downwards if it is cold), maintained at constant temperature, T_w , and immersed in a dilatible fluid (with thermal expansion coefficient α), at temperature T_∞ far from the wall, in a gravity field, g , giving rise to a boundary-layer flow of thickness δ , which starts at the entry border and grows along the length of the plate, with the longitudinal velocity growing from $u=0$ at the wall, to a maximum value within the boundary layer, and finally decreasing to $u=0$ at the outer edge of the layer (Fig. 5); the outer fluid is at rest except for the very small entrainment flow implied by the boundary layer growth.

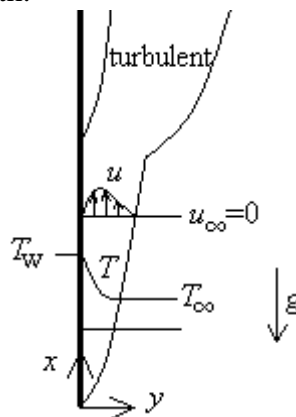


Fig. 5. Boundary layer flow near a vertical plate (one side); notice the choice of x and y coordinates.

The analysis of this boundary-layer flow entirely follows the study made aside for the [forced convection over a flat plate](#). As before, the initial orderly shear flow (laminar flow), after some length usually taken to be $L_{tr} \approx 10^3 [\nu a / (g \alpha \Delta T)]^{1/3}$ (i.e. corresponding to $Ra = 10^9$), transforms into a less-ordered turbulent flow with random velocity-fluctuations, with a thicker boundary layer and a much thinner laminar boundary layer remaining close to the wall (Fig. 5).

The equations governing the flow near the vertical plate, assumed steady and incompressible except for the momentum buoyancy term (Boussinesq model), are the following (notice the choice of coordinates in Fig. 5, for similarity with the [forced boundary layer problem studied before](#)):

- Mass balance (continuity):

$$\nabla \cdot \vec{v} = 0 \rightarrow \frac{\partial u}{\partial x} + \frac{\partial v}{\partial y} = 0 \rightarrow \frac{u_m}{L} \approx \frac{v_m}{\delta} \quad (20)$$

where u_m and v_m are maximum or mean velocity values (here we do not have an imposed value u_∞), showing, as before, that the velocity field is basically one-dimensional.

- Momentum balance:

$$\begin{aligned} \frac{D\vec{v}}{Dt} &= -\frac{\nabla p}{\rho} - g[1 - \alpha(T - T_\infty)]\vec{i}_z + \nu \nabla^2 \vec{v} \rightarrow \\ u \frac{\partial u}{\partial x} + v \frac{\partial u}{\partial y} &= g\alpha(T - T_\infty) + \nu \frac{\partial^2 u}{\partial y^2} \rightarrow \frac{u_m^2}{L} \approx g\alpha(T - T_\infty) \quad \text{or} \quad g\alpha(T - T_\infty) \approx \nu \frac{u_m}{\delta^2} \quad (21) \end{aligned}$$

since one cannot say a priori which term, u_m^2/L or $\nu u_m/\delta^2$ (continuity shows that the two convective terms are of the same order) should balance the driving term here, $g\alpha\Delta T$.

- Energy balance:

$$\frac{DT}{Dt} = a\nabla^2 T + \frac{\phi}{\rho c_p} \rightarrow u \frac{\partial T}{\partial x} + v \frac{\partial T}{\partial y} = a \frac{\partial^2 v}{\partial y^2} \rightarrow u_m \frac{\Delta T}{L} \approx a \frac{\Delta T}{\delta_T^2} \quad (22)$$

since, again, continuity shows that the two convective terms are of the same order). The energy balance gives the order of magnitude of the velocities generated, u_m , and its substitution in the momentum balance (in the first of the two comparisons in (21)):

$$\frac{u_m^2}{L} \approx g\alpha(T - T_\infty) \xrightarrow{u_m \approx aL/\delta_T^2} \frac{a^2 L}{\delta_T^4} \approx g\alpha(T - T_\infty) \quad (23)$$

shows the convenience of defining the so called Rayleigh number Ra , and finally gives:

$$Nu \approx (Ra Pr)^{1/4} \quad \text{with} \quad Ra \equiv \frac{g\alpha(T - T_\infty)L^3}{\nu a} \approx \frac{a}{\nu} \left(\frac{L}{\delta_T} \right)^4 \quad (24)$$

since the Nusselt number is $Nu \equiv hL/k \approx L/\delta_T$. If the second of the two comparisons in (21) had been followed, the result would had been $Nu \approx Ra^{1/4}$ instead of $Nu \approx (Ra Pr)^{1/4}$. The difference between the two comparisons is that the first one in (21) is valid for $Pr \ll 1$ (liquid metals), for which a more accurate correlation is $Nu = 0.57(Ra Pr)^{1/4}$, whereas the second one applies for $Pr \gg 1$ (in practice good enough for $Pr > 0.7$), where a more accurate correlation is $Nu = 0.59 Ra^{1/4}$, valid in the range $10^4 < Ra < 10^9$. A compilation of correlations is later shown in Table 3.

Simon Ostrach found in 1953 an exact solution to the laminar flow near a hot vertical plate, in a similar manner as Blasius' solution for the forced boundary-layer flow, by introducing a self-similar variable, η , defined now by:

$$\eta \equiv \frac{y}{x} \left(\frac{Gr_x}{4} \right)^{1/4}, \quad \text{with} \quad Gr_x \equiv \frac{g\alpha(T-T_\infty)x^3}{\nu^2} \quad (25)$$

where Gr is the so-called Grashof number ($Ra=GrPr$). This similarity variable transforms the PDE system (continuity, momentum, and energy equations) into an ordinary differential equation system in two auxiliary functions, f and θ , f being related to the stream function, $\psi(x,y)=f(\eta)(4\nu(Gr_x/4)^{1/4})$, such that $u=\partial\psi/\partial y$ and $v=-\partial\psi/\partial x$, and θ being $\theta(\eta)\equiv(T-T_\infty)/(T_w-T_\infty)$. Similarly to [Eq. \(21\) in forced-flow boundary layer](#), now one gets:

$$\left. \begin{aligned} \frac{d^3 f}{d\eta^3} + 3f \frac{d^2 f}{d\eta^2} - 2 \left(\frac{df}{d\eta} \right)^2 + \theta &= 0, \quad \text{with} \quad f|_{\eta=0} = 0, \quad \left. \frac{df}{d\eta} \right|_{\eta=0} = 0, \quad \left. \frac{df}{d\eta} \right|_{\eta=\infty} = 0 \\ \frac{d^2 \theta}{d\eta^2} + 3Pr f \frac{d\theta}{d\eta} &= 0, \quad \text{with} \quad \theta|_{\eta=0} = 1, \quad \left. \frac{d\theta}{d\eta} \right|_{\eta=\infty} = 0 \end{aligned} \right\} \quad (26)$$

which, although not analytically integrable, has a universal solution numerically computed, and if the Pr -dependence is empirically fitted, one gets (see Fig. 5):

$$\frac{\delta(x)}{x} = \frac{f_1(Pr)}{Gr_x^{1/4}}, \quad \text{with} \quad f_1(Pr) = \frac{3.93(0.95 + Pr)^{1/4}}{\sqrt{Pr}} \quad (27)$$

what means a $\delta(x) \propto x^{1/4}$ growth-rate for the boundary-layer thickness. In a similar way, fitting the lowest-degree polynomial $u(y)=c_0+c_1y+c_2y^2+c_3y^3$ to the boundary conditions $u(0)=0$, $u(\delta)=0$, and $u'(\delta)=0$, one gets:

$$\frac{u(x,y)}{\nu/x} = f_2(Pr) \sqrt{Gr_x} \frac{y}{\delta(x)} \left(1 - \frac{y}{\delta(x)} \right)^2, \quad \text{with} \quad f_2(Pr) = \frac{5.17}{\sqrt{(0.95 + Pr)}} \quad (28)$$

i.e. a cubic profile for the longitudinal speed. And for the temperature conditions, $T(0)=T_0$, $T(\delta)=T_\infty$, a parabolic profile is good enough:

$$\frac{T(x,y)-T_\infty}{T_w-T_\infty} = \left(1 - \frac{y}{\delta(x)} \right)^2 \quad (29)$$

Finally, the heat-transfer rate in terms of Nusselt number is:

$$Nu_x = f_3(Pr)Gr_x^{1/4}, \quad \text{with} \quad f_3(Pr) = \frac{0.53\sqrt{Pr}}{(0.61 + 1.22\sqrt{Pr} + 1.24Pr)^{1/4}} \quad (30)$$

The above solution applies to all Prandtl numbers (including liquid metals) within the laminar regime, usually valid up to $Ra \approx 10^9$, beyond which the layer becomes turbulent.

Sometimes, natural convection superposes to forced convection and, when both are of similar magnitude, the motion strongly depends on whether they oppose or contribute to each other. For external flow with $Pr \leq 1$, the parameter Gr/Re^2 marks which type of convection is dominant: natural if $\ll 1$, mix if ≈ 1 and forced if $\gg 1$. Often, the Graetz number, $Gz \equiv RePrD/L$, is introduced in mix-convection correlations.

Empirical correlations for natural convection

A small tilting in the hot vertical plate analysed before, already causes great changes in the flow, since the boundary layer detaches at several places along the upper side of the plate (if hot; the lower side in a cold plate), forming three-dimensional patches due to flow instabilities. That is why most heat and mass natural-convection correlations are empirical fittings from experimental data. Table 3 gives a compilation.

Table 3. Convective heat correlations for natural convection.

<i>Configuration</i>	<i>Heat convection</i>
<u>Isothermal vertical wall, laminar flow</u> $Ra_x < 10^9$, any Pr .	$Nu_x = \frac{0.53Pr^{1/4}}{(0.61 + 1.22\sqrt{Pr} + 1.24Pr)^{1/4}} Ra_x^{1/4}$
<u>Isothermal vertical wall, laminar or turbulent flow</u> , any Ra , any Pr (Churchill-Chu-1975), $Nu_L \equiv \int Nu_x dx/L$, also valid for vertical cylindrical walls up to $\delta(x) < D/2$, i.e. if $L/D < Gr_L^{1/4}/35$, both for internal and external flows.	$Nu_L = \left(0.825 + \frac{0.387Ra_L^{1/6}}{\left(1 + \left(\frac{0.492}{Pr} \right)^{9/16} \right)^{8/27}} \right)^2$ Limited range: $Nu_L = 0.59Ra_L^{1/4}$ if $Pr > 0.6$ and $10^4 < Ra < 10^9$ $Nu_L = 0.1Ra_L^{1/3}$ if $Pr > 0.6$ and $10^9 < Ra < 10^{13}$
<u>Isothermal inclined wall:</u> Hot lower side: as vertical but with $g \rightarrow g\cos\theta$ ($\theta < 60^\circ$) Hot upper side with detached plumes, smaller convection. Cold upper side: as vertical but with $g \rightarrow g\cos\theta$ ($\theta < 60^\circ$) Cold lower side with detached plumes, smaller convection.	
<u>Isothermal horizontal wall (upper or lower side)</u> The characteristic length, L , is the exposed area divided by the perimeter, $L \equiv A/p$. Notice that, for a one-side heated horizontal plate, nearly twice as much heat can be	Heat convected from hot upper side, or cold lower side: $Nu_L = 0.54Ra_L^{1/4}$ if $10^4 < Ra < 10^7$ $Nu_L = 0.15Ra_L^{1/3}$ if $10^7 < Ra < 10^{11}$ Heat convected from cold upper side, or hot lower side: $Nu_L = 0.27Ra_L^{1/4}$ for $10^5 < Ra < 10^{11}$

<p>dissipated if the heated side is the upper one.</p> <p><u>Horizontal cylinder (external flow)</u></p>	<p>$Ra_D < 10^9$ (laminar flow), $Pr > 0.7$ (McAdams-1954): $Nu_D = 0.53 Ra_D^{1/4}$ $Ra_D > 10^9$ (turbulent flow), $Pr > 0.7$ (McAdams-1954): $Nu_D = 0.13 Ra_D^{1/3}$ $Ra_D < 10^9$ (laminar flow), $Pr < 0.01$ (Hyman et al.-1953): $Nu_D = 0.53 (Ra_D Pr)^{1/4}$ $Ra_D < 10^{12}$, any regime, any Pr (Churchill-Chu-1975): $Nu_D = \left(0.6 + \frac{0.387 Ra_D^{1/6}}{\left(1 + \left(\frac{0.56}{Pr} \right)^{9/16} \right)^{8/27}} \right)^2$</p>
<p><u>Vertical duct (internal flow). Chimneys</u></p> $\overline{Ra} \equiv \frac{g \alpha (T - T_\infty) R^4}{\nu a L} < 10^5$ <p>and $Pr \approx 1$. R is hydraulic radius, L is height.</p>	$Nu_R = \left[\left(\frac{\overline{Ra}}{C} \right)^m + \left(0.8 \overline{Ra}^{1/4} \right)^m \right]^{1/m}$ <p>Circular duct (radius R): $C=16$, $m=-1$. Square duct (side $s=2R$): $C=14$, $m=-1$. Slot duct (gap width $w=R$): $C=24$, $m=-2$.</p>
<p><u>Sphere (external flow)</u></p> <p>$Ra_D < 10^{11}$, any $Pr > 0.5$ (Churchill-1983).</p>	$Nu_D = 2 + \frac{0.59 Ra_D^{1/4}}{\left(1 + \left(\frac{0.47}{Pr} \right)^{9/16} \right)^{4/9}}$
<p><u>Sphere (internal flow)</u></p> <p>$Pr > 0.5$ (Kreith-1970).</p>	$Nu_D = 0.59 Ra_D^{1/4} \quad \text{for } 10^4 < Ra_D < 10^8$ $Nu_D = 0.13 Ra_D^{1/3} \quad \text{for } 10^9 < Ra_D < 10^{12}$
<p><u>Horizontal rectangular enclosure</u></p> <p>(Internal steady flow, with two opposite adiabatic walls, and a ΔT between the other two walls at separation L, and $Nu_L \equiv hL/k$):</p> <ul style="list-style-type: none"> -Heated from above (stable gradient; no fluid-flow; $Nu_L=1$) -Heated from below with $Ra_D < 1708$, (no fluid-flow; $Nu_L=1$) -Heated from below with $1708 < Ra_D < 10^8$ and $Pr > 0.7$, (flow instability; onset of convection at $Ra_D=1708$). 	$Nu_L = 1 + 1.44 \left[1 - \frac{1708}{Ra_L} \right]^+ + \left[\frac{Ra_L^{1/3}}{18} - 1 \right]^+$ <p>[]⁺ means that these terms must only be accounted if positive (set to 0 if negative). Holland et al. (1976).</p>
<p><u>Vertical rectangular enclosure</u></p> <p>(Internal steady flow, with a ΔT between the two vertical walls at separation L, and the adiabatic walls at separation H), $Nu_L \equiv hL/k$.</p>	<p>$1 < H/L < 2$, any Pr, $Ra_L > 10^3(0.2+Pr)/Pr$:</p> $Nu_L = 0.18 \left(\frac{Pr Ra_L}{0.2 + Pr} \right)^{0.29}$ <p>$2 < H/L < 10$, any Pr, $Ra_L < 10^{10}$:</p> $Nu_L = 0.22 \left(\frac{Pr Ra_L}{0.2 + Pr} \right)^{0.28} \left(\frac{L}{H} \right)^{0.25}$ <p>$10 < H/L < 40$, any $Pr > 1$, $10^4 < Ra_L < 10^7$:</p> $Nu_L = 0.42 Ra_L^{0.25} Pr^{0.012} \left(\frac{L}{H} \right)^{0.3}$

<p>Inclined rectangular enclosure (Internal steady flow, with a ΔT between the two closest walls at separation L, tilted an angle θ from the vertical, and the adiabatic walls at separation H), $Nu_L \equiv hL/k$. Fluid flow changes beyond a critical angle $\theta_{cr}(H/L)$:</p> <table border="1" data-bbox="150 456 759 539"> <thead> <tr> <th>$H/L =$</th> <th>1</th> <th>3</th> <th>6</th> <th>12</th> <th>>12</th> </tr> </thead> <tbody> <tr> <td>θ_{cr}</td> <td>25°</td> <td>53°</td> <td>60°</td> <td>67°</td> <td>70°</td> </tr> </tbody> </table>	$H/L =$	1	3	6	12	>12	θ_{cr}	25°	53°	60°	67°	70°	<p>$0 < \theta < \theta_{cr}, H/L < 12, Pr > 0.7$</p> $Nu_{\theta} = Nu_{\theta=0} \left(\frac{Nu_{\theta=0}}{Nu_{\theta=90^{\circ}}} \right)^{\theta/\theta_{cr}} (\sin \theta_{cr})^{\frac{\theta}{4\theta_{cr}}}$ <p>$0 < \theta < \theta_{cr}, H/L \geq 12, Pr > 0.7$</p> $Nu_{\theta} = 1 + 1.44 \left[1 - \frac{1708}{Ra_L \cos \theta} \right]^+ \left(1 - \frac{1708 (\sin(1.8\theta))^{1.6}}{Ra_L \cos \theta} \right) + \left[\frac{(Ra_L \cos \theta)^{1/3}}{18} - 1 \right]^+$ <p>$\theta_{cr} < \theta < 90^{\circ}, \text{ any } H/L, Pr > 0.7$</p> $Nu_{\theta} = Nu_{\theta=90^{\circ}} (\sin \theta)^{1/4}$
$H/L =$	1	3	6	12	>12								
θ_{cr}	25°	53°	60°	67°	70°								
<p>Concentric cylindrical enclosure (internal steady flow, with a ΔT between the two surfaces, with axial width W), $L \equiv (D_o - D_i)/2, \dot{Q} = \frac{2\pi k_{eff} W \Delta T}{\ln(D_o/D_i)}$ $Pr > 0.7, 10^2 < F_{cyl} Ra_L < 10^7$ ($k_{eff} = k$ for $< 10^2$)</p>	$\frac{k_{eff}}{k} = 0.386 \left(\frac{Pr F_{cyl} Ra_L}{0.86 + Pr} \right)^{1/4},$ $F_{cyl} \equiv \frac{8 [\ln(D_o/D_i)]^4}{(D_o - D_i)^3 (D_i^{-3/5} - D_o^{-3/5})^5}$												
<p>Concentric sphere enclosure (internal steady flow, with a ΔT between the two surfaces), $L \equiv (D_o - D_i)/2, \dot{Q} = \frac{2\pi k_{eff} D_o D_i \Delta T}{D_o - D_i}$ $Pr > 0.7, 10^2 < F_{sph} Ra_L < 10^4$ (if $< 10^2, k_{eff} = k$)</p>	$\frac{k_{eff}}{k} = 0.74 \left(\frac{Pr F_{sph} Ra_L}{0.86 + Pr} \right)^{1/4},$ $F_{cyl} \equiv \frac{D_o - D_i}{2 (D_o D_i)^4 (D_i^{-7/5} - D_o^{-7/5})^5}$												

Empirical correlations for other configurations can be found in the literature; e.g. other enclosure geometries, combined natural and forced convection, convection in fix porous media, convection in fluidized beds, convection in vibrating systems, convection with very high velocities, convection in rarefied gases, etc. [Convection with phase change](#), and [Heat exchangers](#), are separately considered.

Heat transfer fluids

There is a great variety of fluids used to convect excess of deficit of thermal energy from an origin location (source) to a destination location (sink). According to the purpose (temperature difference) there are two possible applications (might be thought of as high-T and low-T fluids, relative to T-environ):

- Heating fluids (used to heat up a load by convection).
- Cooling fluids (used to cool loads). The word '[coolant](#)' is often used for cooling fluids and, by extension, to design any heat transfer fluid.

Heat transfer fluids can be grouped according to their properties as:

- [Gases](#). Air is by far the most common heat transfer fluid.
- [Liquids](#). Water is the first choice, but it has some handicaps that may require other working fluids; e.g. water cannot be used below 0 °C or above 100 °C (pressurised water may work up to

$T_{tr}=374\text{ °C}$); it is biologically and chemically active (corrosive, prone to contamination), may be electrically conducting (risk of short-circuits), etc.

- Phase-changing fluids. Most liquids may be used as two-phase heat-transfer fluids; the most used are water/steam, ammonia (toxic), hydrocarbons (flammable), and halocarbons.

See Temperature and pressure effects on fluid properties, [aside](#).

Air and other permanent gases

Ambient air is the omnipresent convection fluid in all terrestrial applications, either by natural convection due to buoyancy, or by forced convection with a fan (or within a wind). Any electrical appliance (e.g. the computer I am working with now) serves to illustrate the point.

Air is a free commodity, clean, non-flammable, non-corrosive, and it does not boil or freeze (well, frosting may be a problem with humid air, and any fluid would condense at a low-enough temperature). However, it has a very low thermal conductivity and density. Hydrogen or helium are used when higher conductivity gases are needed. Sulfur hexafluoride, SF_6 , is used for cooling and insulating of some high-voltage power systems (circuit breakers, switches, some transformers, etc.).

Water

Tap water is much used as a heat transfer fluid because of its availability and good thermal properties: it has good thermal conductivity, a large thermal capacity, low viscosity, and presents no hazard (usually just a spillage problem). Unfortunately, its operating range poses some restrictions at high temperatures (can only work up to 100 °C at normal pressure, and up to 370 °C at some 22 MPa), and a severe restrictions at low temperatures (can only work down to 0 °C , with negligible pressure-influence). Besides, natural solutes like dissolved gases and salts may have detrimental effects (e.g. corrosion and depositions). To palliate these problems, distilled water can be used.

Water antifreeze mixtures

To solve the lower-range operating-temperature handicap of pure water, several antifreeze mixtures are commonly used, as water/alcohol mixtures (water/propylene-glycol or water/ethylene-glycol, the latter being toxic), and water/salt brines. A detailed study can be found in [Solutions](#).

Silicone oils

Silicone oils are poly-dimethyl-siloxanes, oily synthetic fluids with a very wide operating temperature range (say from -40 °C to 320 °C), and a wide range of viscosities. They are non-corrosive and long-lasting. However, their thermal conductivity and thermal capacity are poor.

Hydrocarbon oils

They started to be high-temperature distillates from crude-oil, but most of the present mineral oils are synthetic. Hydrocarbon oils are very good at high operating temperatures (they can work say from -30 °C to 400 °C), but a higher viscosity and lower thermal capacity than water.

Fluorocarbon oils

Fluorocarbons (FC, also named perfluorocarbons, PFC), are synthetic halocarbons with just fluorine as halogenating atom. They show remarkable properties as thermal, chemical, and biological stability, i.e. wide useful temperature range, good phase-change properties, non-corrosive, electrical insulation, etc.

Phase-change fluids. Refrigerants

Most liquids may be used as two-phase heat-transfer fluids. We restrict here to phase changes between fluid phases (for fluid-to-solid phase-change materials, [PCM](#), see [Hot pads and cold pads](#)), and in particular to refrigerant fluids (working fluids used in [refrigeration and heat pumps](#)).

The working substances most used in refrigeration are:

- Synthetic refrigerants, better known as halogenated hydrocarbons, from the old and retired chlorofluorocarbons (CFC), to hydrochlorofluorocarbons (HCFC), hydrofluorocarbons (HFC), and perfluorocarbons (PFC).
- Natural refrigerants, usually split in:
 - Hydrocarbons (propane, n-butane, iso-butane...); they are flammable.
 - Others, notably ammonia and carbon dioxide.

Liquid metals

Liquid metals have thermal conductivity one or two orders of magnitude larger than common liquids, but its use poses severe technological problems, a major one being the scarcity of suitable liquid metals for work at room temperatures; practically the only important application of liquid metals as heat convection fluids is the sodium-potassium mixture used in nuclear-engineering cooling.

Nanofluids

A new approach to enhance heat convection is to use a colloidal dispersions of solid particles (in the nanometric range, i.e. $d < 10^{-7}$ m) into ordinary liquids, what is named 'nanofluids'. The small particle size prevents settling and clogging, and the apparent thermal transmittance of the fluid gets highly improved even when minute concentrations are used, particularly in the laminar range, the reason being still unclear. Typical nanoparticles used are carbon derivatives (graphite, carbon nanotubes, metal carbides), metallic oxides (Al_2O_3 , CuO , TiO_2 ...), in both cases up to 5% in weight concentration, or pure metals (Cu, Al, Ag, Au...) in much smaller concentrations (<0.1%). Base liquids may be water, antifreezers, oils, or bio-fluids. Some additive to stabilise the dispersion may be needed (e.g. succinonitrile is added to stabilise carbon-nanotubes in oils). Heat-transfer enhancement grows with particle concentration (typically up to 50% of the base fluid at room temperature), and increases with operating temperature.

[Back to Heat and mass transfer](#)

[Back to Thermodynamics](#)